

## Green Synthesis and Characterisation of Ag<sub>2</sub>O and Ag<sub>2</sub>O-Ce<sup>3+</sup> nanoparticles

Varadaraju V D<sup>1</sup>, Bharath Narasimha Y R<sup>2</sup>, H N Shivananjaiah<sup>3\*</sup>

<sup>1-3</sup>Department of PG studies in Chemistry, Nrupathunga University, Nrupathunga road, Bangalore - 560001, Karnataka, India.

### ABSTRACT

Nanoparticles are usually defined as particles of matter that are between 1 and 100 nm in diameter. Silver oxide nanoparticles have a wide range of applications and they are usually used as sensors, catalysts, optical probes, and in the medicinal field. Nanoparticles of undoped and cerium-doped silver oxide nanoparticles are synthesized using the combustion method while using the latex of jackfruit as fuel (Green synthesis). Crystalline properties and optical properties of the samples were determined using the X-ray diffraction method, UV-visible spectroscopy method, IR spectroscopy method, Scanning electron microscope, and particle analysis. Average particle size was determined by X-ray diffraction method, functional groups were determined by using IR spectroscopy, and the concentration of functional groups was determined by UV-visible spectroscopy. This characterization could be used to study the difference between undoped silver oxide nanoparticles and cerium-doped silver oxide nanoparticles.

**Keywords:** Nanoparticles, Doped, Spectroscopy, X-ray diffraction, UV-visible, FTIR, Particle analysis, Jack fruit (*Artocarpus Heterophyllus*), Green synthesis.

### 1. INTRODUCTION

A nanoparticle is usually defined as a particle that is between 1 and 100 nanometres in diameter (1). Being smaller than the wavelength range of visible light which is 400-700 nm nanoparticles cannot be seen through ordinary microscopes therefore electron microscopes are used (2). The small size and high surface-to-volume ratio are the two important properties that help in modifying the physical and chemical properties of nanoparticles (3)(4).

**Silver Oxide (Ag<sub>2</sub>O) nanoparticles** are spherical of high surface area oxide magnetic nanostructured particles. Nanoscale Silver Oxide Particles are typically 20-80 nanometers (nm) with a specific surface area (SSA) in the 10 - 50 m<sup>2</sup>/g range and also available with an average particle size of 100 nm range with a specific surface area of approximately 7- 10 m<sup>2</sup>/g. Nano Silver Oxide particles are also available in ultra-high purity and high purity, transparent, coated and dispersed forms(8).

Silver oxide nanoparticles are used as sensors, optical probes, antibacterial agents and antimicrobial agents, and as catalysts. The combustion method is a material preparation method that is simple economical and flexible. Energy necessities are only required in the initial step since the ideal products are obtained by utilizing heat generated by exothermic reactions between reactants (9).

The edible pulp is 74% water, 23% carbohydrates, 2% protein, and 1% fat. The carbohydrate component is primarily sugars and is a source of dietary fiber. In a 100-gram (3+1/2-ounce) portion, raw jackfruit provides 400 kJ (95 kcal) and is a rich source (20% or more of the Daily Value, DV) of vitamin B<sub>6</sub> (25% DV). It contains moderate levels (10-19% DV) of vitamin C and potassium, with no significant content of other micronutrients. The jackfruit is a partial solution for food security in developing countries. (10)(11)

### 2. MATERIALS AND METHODS

**2.1. Materials:** Silver nitrate, Cerium nitrate, Jack fruit latex, water, magnetic stirrer, Muffle furnace(14).

#### 2.2. Synthesis:

- Plant extract of jack fruit is collected by collecting the latex from jack fruit from the surroundings of Bangalore and then stored in the fridge for some time. Then the latex is mixed with 100 ml of

water and kept in a magnetic stirrer for about 3 hours to reduce the viscosity and sticky nature of the latex to turn it into a milk-like solution (15).

- In the solution combustion method, the reaction mixture was prepared by adding 10ml of the plant extract and silver nitrate as a source of silver. The reaction was kept in a pre-heated muffle furnace maintained at 270<sup>0</sup>C, where Ag<sub>2</sub>O nanoparticles are formed within 3 hours. The obtained products of Ag<sub>2</sub>O nanoparticles were stored in an airtight container for further analysis.

Ag<sub>2</sub>O-Ce<sup>3+</sup> nanoparticles were also prepared by the same method.

**Synthesis of Ag<sub>2</sub>O and Ag<sub>2</sub>O-Ce<sup>3+</sup> nanoparticles with different concentrations by combustion method.**

Serial number	Cerium concentration in %	AgNO <sub>3</sub> in gram	Ce (NO <sub>3</sub> ) <sub>3</sub> in gram
1	0	0.170	0
2	1%	0.1683	0.0017
3	2%	0.1666	0.0034
4	3%	0.1649	0.0051

### Synthesis of 1% compound

Exactly 0.1683 g of silver nitrate and 0.0017 g of cerium nitrate were dissolved in 10 ml of plant extract which gives 1% solution. This mixture is taken in a silica crucible and kept in a pre-heated muffle furnace heated at 270-300<sup>0</sup>C. Above 300<sup>0</sup>C nanoparticles cannot be obtained as nanoparticles will be vapourised.

Similarly, 2%, and 3% concentrations were prepared accordingly.

## 3. CHARACTERISATION

### 3.1. Powder X-ray diffraction method

This method is used to determine the crystalline size, crystal structure, interplanar spacing, and crystal lattice strain. The sample of undoped silver oxide nanoparticles and cerium doped nanoparticles which is obtained from synthesis is placed in PW-1840 Philips X-ray diffraction at room temperature using Cu K $\alpha$  radiation emitter of wavelength  $\lambda=1.542\text{\AA}$  and X-ray is made to an incident on it. The scattered X-ray constructively produces a diffraction beam which is analyzed.

### 3.2. Fourier transform infrared spectroscopy (FTIR)

This method is used to determine functional groups. On interaction with the sample of undoped silver oxide nanoparticles and cerium doped nanoparticles which is obtained from synthesis, the sample tends to absorb radiation of a specific frequency. The remaining light, which is not absorbed by groups of atoms, is transmitted through the sample to a detector. Here the transmitted light is analyzed and the frequencies absorbed by the material are determined. The resulting plot of absorbed energy versus frequency is called the infrared spectrum. After this, the signal is converted mathematically (Fourier transform) into the classical spectrum and the spectral absorption of a sample is scanned. This technique is known as Fourier transform infrared spectroscopy.

### 3.2. Scanning electron microscopy (SEM)

This method is used to determine the surface topography and composition of the sample. SEM images have a 3-D appearance and are useful for studying the surface structure of the sample. In this method, the images are obtained by focusing the electron beam on the sample which produces various signals which contain the surface topography and composition of the sample.

### 3.3. UV-visible spectroscopy

This method is used to determine the concentration of functional groups in the sample. The sample of undoped silver oxide nanoparticles and cerium doped nanoparticles which is obtained from synthesis is placed UV spectrometer where UV rays are made to an incident on it which gives a UV spectrum that is analyzed. Measurement of the attenuation of a beam of light after it passes through a sample or after reflection from a sample surface. The attenuation can result from absorption,

scattering, reflection or inflection, or interference. Experimental measurements are made in terms of T:  $T=I/I_0$ .

#### 4. RESULTS AND DISCUSSIONS

##### 4.1. X-ray diffraction studies

The X-ray diffraction pattern of  $Ag_2O$  and  $Ag_2O-Ce^{3+}$  nanoparticles from silver nitrate, Cerium nitrate, and jackfruit latex as biofuel at  $270^{\circ}$ - $300^{\circ}C$  is shown in the figure. The XRD patterns revealed the orientation and crystalline nature of  $Ag_2O$  and  $Ag_2O-Ce^{3+}$  nanoparticles. From (Fig 4.1.1) the diffraction peaks situated at  $38.2^{\circ}$ ,  $44.4^{\circ}$ ,  $64.6^{\circ}$ ,  $77.5^{\circ}$  and  $81.7^{\circ}$  which can be indexed to (111), (200), (220), (311), and (222) planes respectively give you the evidence of  $Ag_2O$  nanoparticles. From (Fig 4.1.2) the diffraction peaks at  $2\theta$  values 28.85 matched with (222) giving you evidence of  $Ag_2O-Ce^{3+}$  nanoparticles. The average crystallite size was calculated using the Debye-Scherrer equation.

$$D = \frac{k\lambda}{\beta \cos\theta}$$

Where, D=crystallite size of silver oxide nanoparticles,  $\lambda$ =wavelength of x-ray source (0.151nm used in XRD),  $\beta$ =full width at half maximum of the diffraction peak, k=Scherrer constant (0.9 to 1 nm),  $\theta$ =Brag's angle. The average particle size obtained from XRD data is found to be about 37.90 nm.

Sample 1

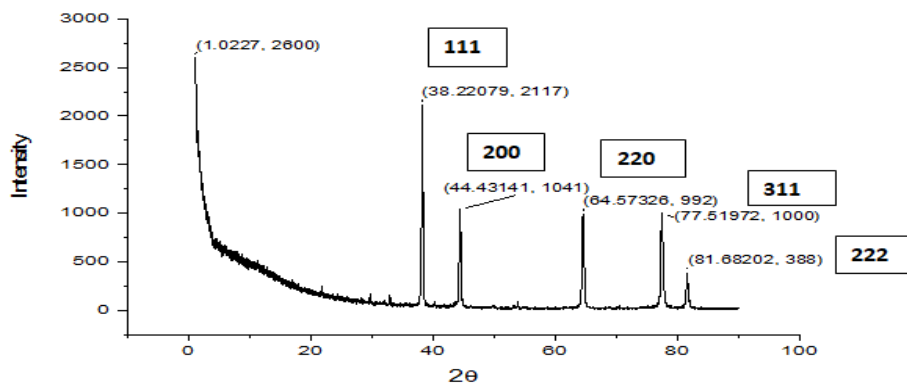


Fig 4.1.1. XRD pattern of undoped  $Ag_2O$ .

Sample 2

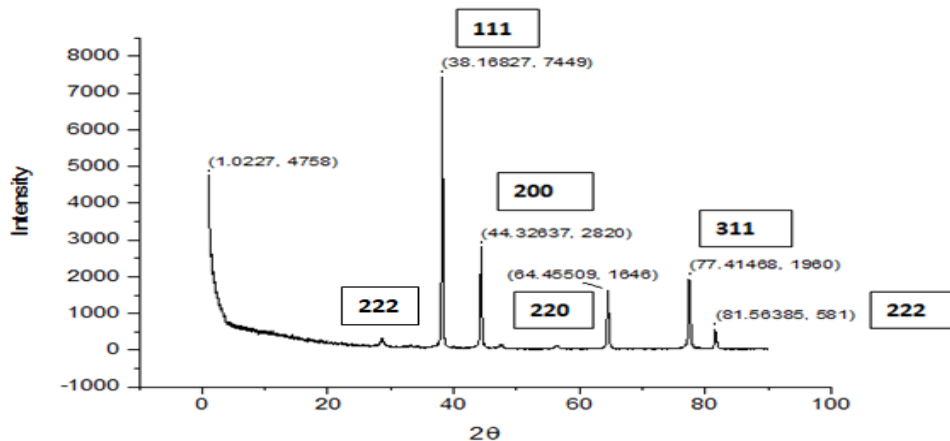


Fig 4.1.2. XRD pattern of 1% Ce doped  $Ag_2O$ .

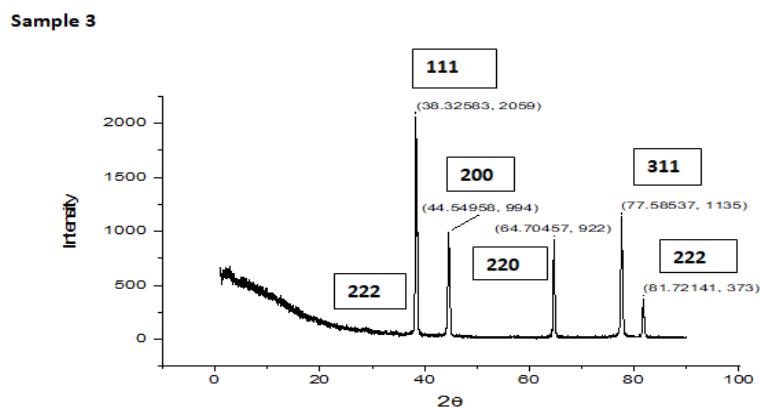


Fig 4.1.3. XRD pattern of 2% Ce doped Ag<sub>2</sub>O.

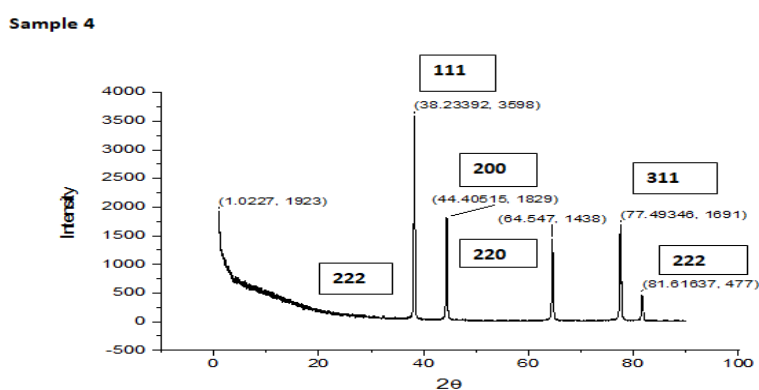


Fig 4.1.4. XRD pattern of 3% Ce doped Ag<sub>2</sub>O.

#### 4.2. Fourier transform infrared spectroscopy (FTIR)

The FTIR spectrum of the Ag<sub>2</sub>O and Ag<sub>2</sub>O-Ce<sup>3+</sup> nanoparticles is shown in the figure from (Fig 4.2.1) the synthesized Ag<sub>2</sub>O nanoparticles show the infrared in the region 1988, 1913, 1853, 1612, 1535, 1294, 1043, 800, 569, 536 cm<sup>-1</sup>. from (fig 4.2.2) for Ag<sub>2</sub>O-Ce<sup>3+</sup> (1% Ce) nanoparticles show the infrared absorption in the region 2908, 1354, 1219, 1076, 773, 682, 640 cm<sup>-1</sup>. From Fig 4.2.3 for Ag<sub>2</sub>O-Ce<sup>3+</sup> (2% Ce) nanoparticles show the infrared absorption in the region 3275, 1923, 1624, 1330, 1219, 1083, 773 cm<sup>-1</sup>. From Fig 4.2.4 for Ag<sub>2</sub>O-Ce<sup>3+</sup> (3% Ce) nanoparticles show the infrared absorption in the region 1988, 1517, 1219, 771, 682, 493, 418 cm<sup>-1</sup>. According to the obtained data, it can be stated that we have successfully synthesized Ag<sub>2</sub>O and Ag<sub>2</sub>O-Ce<sup>3+</sup> nanoparticles using a Muffle Furnace-assisted combustion procedure.

**SAMPLE 1:** The peak observed at 1535 cm<sup>-1</sup> gives N-O stretching, at 1294 cm<sup>-1</sup> gives C-N stretching and at 1043 cm<sup>-1</sup> gives C-O stretching, and at 1988 cm<sup>-1</sup>, 1612 cm<sup>-1</sup> and 1913 cm<sup>-1</sup> gives C=C stretching and at 800 cm<sup>-1</sup> gives C-H stretching.

**SAMPLE 2:** The peak observed at 773.46 cm<sup>-1</sup> gives evidence to aromaticity, 1354.03 cm<sup>-1</sup> and 1219 cm<sup>-1</sup> gives evidence to amines, 682.80 cm<sup>-1</sup> gives alkenes, 640.37 cm<sup>-1</sup> gives alkanes, 2908.65 cm<sup>-1</sup> gives C-H stretching, 1076.20 cm<sup>-1</sup> gives amines C-N stretching.

**SAMPLE 3:** The peak observed at 773.46 cm<sup>-1</sup> and 1624.06 cm<sup>-1</sup> gives evidence to alkenes, 1083.99 cm<sup>-1</sup>, 1219 cm<sup>-1</sup>, and 1330.88 cm<sup>-1</sup> gives evidence to amines, 1923.03 cm<sup>-1</sup> gives evidence to aromaticity, 3275.13 cm<sup>-1</sup> gives evidence to -OH stretching in the carboxylic group.

**SAMPLE 4:** The peak observed at 418.55 gives C-N stretching, 682.80 cm<sup>-1</sup> and 771.53 cm<sup>-1</sup> gives alkenes, 1219.01 cm<sup>-1</sup> gives amines and 1517.88 cm<sup>-1</sup> gives evidence of aromaticity.

The peaks observed at 800.46 cm<sup>-1</sup> in sample 1 and 773.46 cm<sup>-1</sup> in sample 2 and 773.46 cm<sup>-1</sup> in sample 3 and 771.53 cm<sup>-1</sup> in sample 4 gives evidence of Ag<sub>2</sub>O nanoparticles. While the peaks at 2908.65 cm<sup>-1</sup>

<sup>1</sup> in sample 2 and 3275.13 cm<sup>-1</sup> in sample 3 and 1988.61 cm<sup>-1</sup> in sample 4 gives evidence of Ce<sup>3+</sup>-Ag<sub>2</sub>O nanoparticles and change in chemical shift.

**Sample 1**

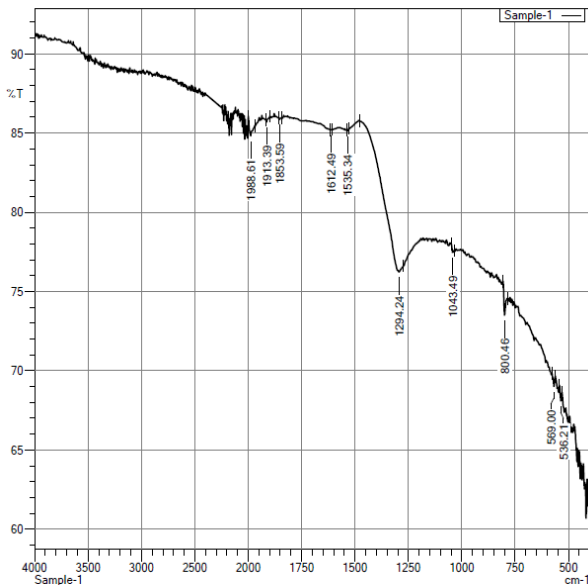


**Fig 4.2.1**

**Sample 2**

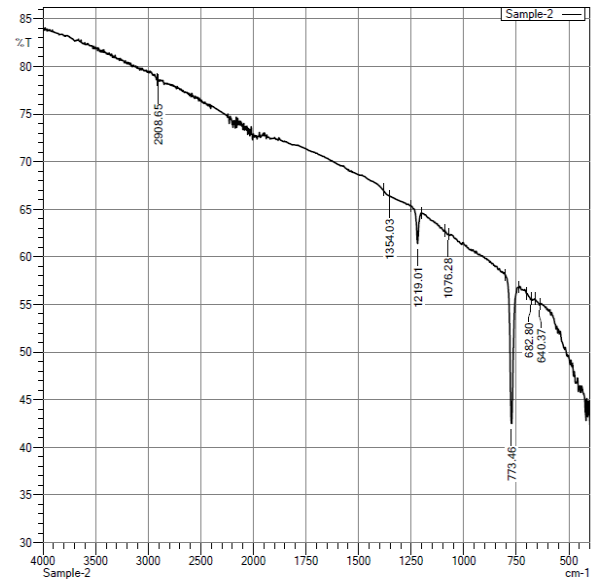


**Fig 4.2.2**

**Fig 4.2.1. FTIR spectra of undoped Ag<sub>2</sub>O, Fig 4.2.2. FTIR spectra of 1% Ce doped Ag<sub>2</sub>O.**

**Sample 3**

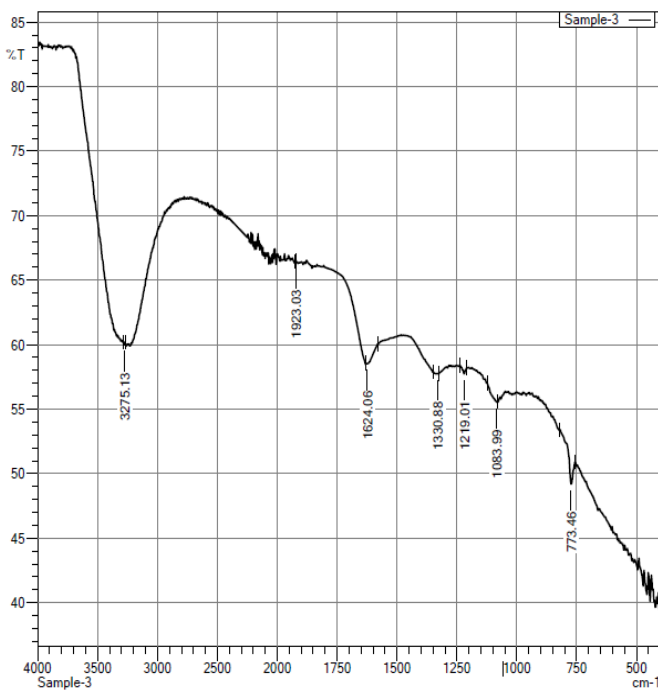


**Fig 4.2.3**

**Sample 4**

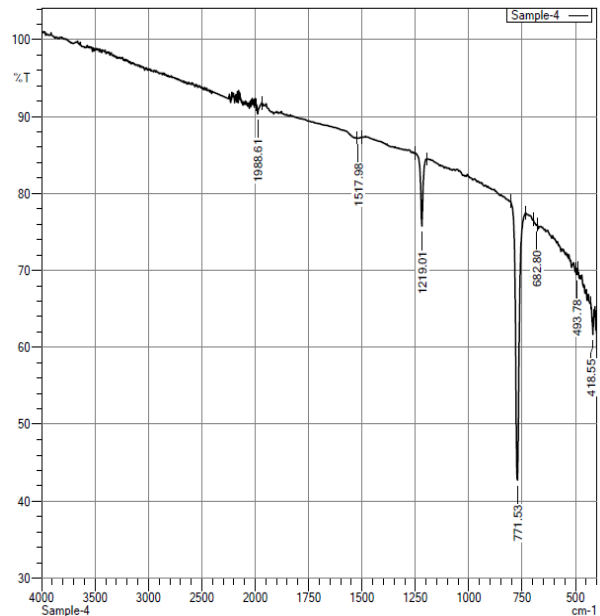


**Fig 4.2.4**

**Fig 4.2.3. FTIR spectra of 2% Ce doped Ag<sub>2</sub>O, Fig 4.2.4. FTIR spectra of 3% Ce doped Ag<sub>2</sub>O.**

### 4.3. UV-visible spectroscopy

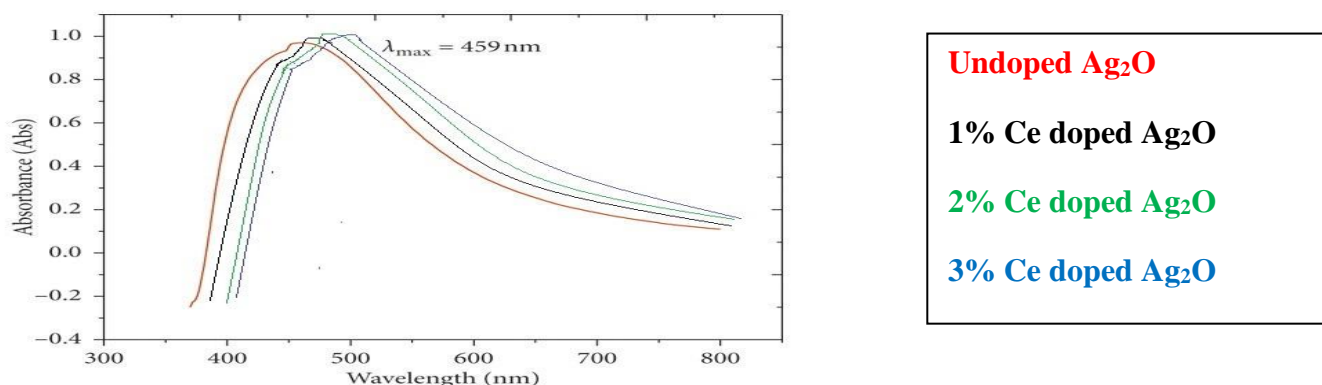


**Fig 4.3.1. UV-visible spectra of Ag<sub>2</sub>O and Ce<sup>3+</sup>Ag<sub>2</sub>O nanoparticles**

From Fig 4.3.1 silver oxide nanoparticles show a chemical shift at 459 nm as a broad peak. The tail part of the broadband extends towards the UV region, attributed to the resonant excitation of surface Plasmon and interband transitions respectively. The single-surface Plasmon peak implies that the particles are spherical in shape. In case of the ellipsoidal particles there exist two Plasmon peaks.

### 4.4. Scanning electron microscopy (SEM)

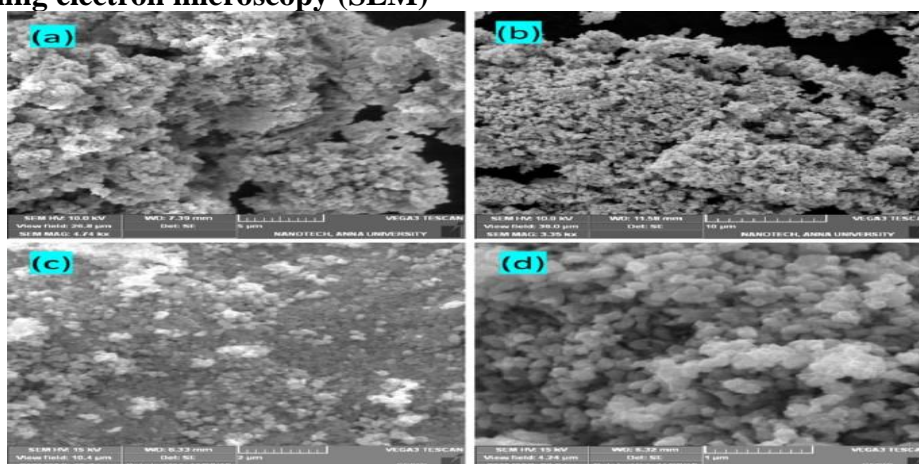


**Fig 4.4.(a). Undoped Ag<sub>2</sub>O, Fig 4.4.(b) 1% Ce doped Ag<sub>2</sub>O, Fig 4.4.(c) 2% Ce doped Ag<sub>2</sub>O, Fig 4.4.(d) 3% Ce doped Ag<sub>2</sub>O.**

According to the SEM analysis of sample 1 Fig 4.4.(a), the morphology was found to be spherical, with particle size 15-84 nm as it varies with the deposition of thin films over different cycles. In sample 2 Fig 4.4.(b), sample 3 Fig 4.4.(c) and sample 4 Fig 4.4.(d) with an increase in cerium concentration silver oxide concentration decreases so particles of size ranging from 24-50 nm were formed.

## 5. CONCLUSION

Undoped silver oxide nanoparticles and cerium-doped silver oxide nanoparticles were prepared through the combustion method using the latex of jackfruit as fuel. The characterization of morphology and chemical properties was done through XRD, FTIR, UV, and SEM analysis. These nanoparticles have a wide variety of applications and future work is focused on the medicinal field.

## 6. ACKNOWLEDGEMENT

I deeply appreciate the help and mentoring from H.N.Shivananjaiah and Dr.Ramakrishna Reddy in PG Department, Nrupathunga University, Bangalore for regular input for this research. Dr.Ashwath Narayan Gowda from Raman Institute for XRD, FTIR, and UV results.

**7. REFERENCE**

- (1) The chemistry of nanomaterials: Synthesis, Properties, and Applications, C.N.R. Rao, A. Muller, A.K. Cheetham, WILEY-VCH Verlag GmbH & Co., **2004**.
- (2) Nanoscale Materials in Chemistry, Kenneth J. Klabunde, Ryan M. Richards, John Wiley & Sons, Inc., Hoboken, New Jersey, **2009**.
- (3) Spring Handbook of Nanotechnology, Bharat Bhushan, Springer Heidelberg Dordrecht London New York, **2010**.
- (4) Nanomaterials: An introduction to synthesis, properties and Application, Dieter Vollath, John Wiley and Sons, **2013**.
- (5) Nanomaterials, Nanotechnologies and Design, Michael F. Ashby, Paulo J. Ferreira, Daniel L.Schodek, Elsevier Ltd., UK, **2009**.
- (6) Introduction to Nanomaterials, A. Alagarasi, **2007**.
- (7) Nanostructures and Nanomaterials: Synthesis, Properties, and Applications, Guozhong Cao, Imperial College Press, Convent Garden, London, **2004**.
- (8) Synthesis and characterization of silver oxide nanoparticles by a Novel Method, Ng Law Yong, Akil Ahmad, Abdul Wahab Mohammad, **2013**
- (9) A Review on Synthesis and Characterization of Ag<sub>2</sub>O Nanoparticles for Photocatalytic Applications, M. Shume, H. C. Ananda Murthy, and Enyew Amare Zereffa, **2020**
- (10) A Review on Importance of Artocarpus heterophyllus L. (Jackfruit) , Ahasan Ullah Khan , Israt Jahan Ema, Md. Ruman Faruk, Shofiul Azam Tarapder. AnayatUllah Khan, Sana Norcen and Muhammad Adnan,**2021**.
- (11) Studies on antibacterial and antifungal activity of silver nanoparticles synthesized using Artocarpus heterophyllus leaf extract , Rebecca Thombre, Fenali Parekh, Parvathi Lekshminarayanan, Glory Francis , **2012**.
- (12) Synthesis, characterization and application of Ag doped ZnO nanoparticles in a composite resin , Hércules Bezerra Diasa,c, Maria Inês Basso Bernardi, Valéria Spolon Marangoni, Adilson César de Abreu Bernardi, Alessandra Nara de Souza Rastelli, Antônio Carlos Hernandez , **2019**.
- (13) Photodegradation of tartrazine dye favored by natural sunlight on pure and (Ce, Ag) co-doped ZnO catalysts , Tayeb Bouarroudj, Lamine Aoudjit, Lerari Djahida, Beddiaf Zaidi, Maamar Ouraghi, Djamilia Zioui, Sarah Mahidine, Chander Shekhar and Khaldoun Bachari , **2021**.
- (14) Green mediated synthesis of lanthanum doped zinc oxide:Study of its structural , optical and latent fingerprint applications , H.N.Shivananjiah , K.Sailaja Kumari , M.S.Geetha, Journal of Rare Earths 38 , **2020** , 1281-1287.
- (15) Green mediated synthesis and characterization of dysprosium doped cadmium oxide nano particles ,H.N.Shivananjiaiah , K.Sailaja Kumari, Research Journal of Chemistry and Environment , 24 , **2020** , 131-135.
- (16) Green mediated synthesis and characterization of ZnO ,H.N.Shivananjiaiah , K.Sailaja Kumari , M.S.Geetha , International Journal of All Research Education and Scientific Methods , 10 , **2020** , 2455-6211.